Lawrence Berkeley National Laboratory
Recent Work

Title
ELASTIC SCATTERING OF 5-BeV n- MESONS ON HYDROGEN

Permalink
https://escholarship.org/uc/item/8v35x8cr

Author
Thomas, Richard G.

Publication Date
1959-11-23

eScholarship.org Powered by the California Digital Library
University of California

UNIVERSITY OF CALIFORNIA

Ernest O. Lawrence Radiation Laboratory

TWO-WEEK LOAN COPY

This is a Library Circulating Copy which may be borrowed for two weeks. For a personal retention copy, call Tech. Info. Division, Ext. 5545

BERKELEY, CALIFORNIA

DISCLAIMER

This document was prepared as an account of work sponsored by the United States Government. While this document is believed to contain correct information, neither the United States Government nor any agency thereof, nor the Regents of the University of California, nor any of their employees, makes any warranty, express or implied, or assumes any legal responsibility for the accuracy, completeness, or usefulness of any information, apparatus, product, or process disclosed, or represents that its use would not infringe privately owned rights. Reference herein to any specific commercial product, process, or service by its trade name, trademark, manufacturer, or otherwise, does not necessarily constitute or imply its endorsement, recommendation, or favoring by the United States Government or any agency thereof, or the Regents of the University of California. The views and opinions of authors expressed herein do not necessarily state or reflect those of the United States Government or any agency thereof or the Regents of the University of California.

For Phys. Rev.

UCRL-8965 Rev

UNIVERSITY OF CALIFORNIA

Lawrence Radiation Laboratory
Berkeley, California

Contract No. W-7405-eng-48

ELASTIC SCATTERING OF 5-BEV π^- MESONS ON HYDROGEN

Richard G. Thomas, Jr.

November 23, 1959

Printed for the U. S. Atomic Energy Commission

ELASTIC SCATTERING OF 5-BEV π^- MESONS ON HYDROGEN

Richard G. Thomas, Jr.

Lawrence Radiation Laboratory
University of California
Berkeley, California

November 23, 1959

ABSTRACT

The elastic scattering of 5-Bev negative pions on hydrogen has been observed in a large propane bubble chamber. We report below the results of this observation. It is shown that $\approx(7 \pm 3)\%$ of the events called elastic are probably background. The observed angular distribution is strongly peaked forward. This fact suggests that diffraction scattering is the dominant process at this energy. The theoretical analysis of the distribution is in terms of the optical model. It is shown that the proton acts like a partially opaque sphere of radius 1.04×10^{-13} cm $\pm$ 5%. The total elastic cross section is found to be 5.6 $\pm$ 0.5 mb. From the extrapolated value of $d\sigma(0)/d\Omega$ = 29.8 $\pm$ 10% in the center-of-mass system, a value of 29.1 $\pm$ 2.9 mb was calculated for the total hydrogen cross section. The opacity of the sphere is thus 0.69 $\pm$ 0.05.

ELASTIC SCATTERING OF 5-BEV π^- MESONS ON HYDROGEN*

Richard G. Thomas, Jr.

Lawrence Radiation Laboratory
University of California
Berkeley, California

November 23, 1959

INTRODUCTION

Since the discovery that pi mesons interact strongly with nucleons,[1] much time has been and is currently being spent studying these interactions. It is now fairly certain that when a satisfactory theory of nuclear forces is enunciated, pions will play a dominant role. Among the many interactions of pions with protons at moderate energies ($\lesssim$ 1 Bev), elastic scattering can be studied most readily. The information that is obtained in one of these experiments usually consists of (a) the pion-proton interaction radius; (b) the angular distribution of the elastically scattered mesons; (c) a test of one or more models of the nucleus; and (d) the total elastic-scattering cross section. The experiment to be described yielded data not only on the above quantities, but also on the total hydrogen cross section. The calculation of this cross section was made on the assumption that the elastic interaction at this energy is almost wholly diffraction scattering. The observed angular distribution is thus treated by the conventional optical model in which the behavior of the nucleon is described by an opaque sphere.[2]

* This work was done under the auspices of the U. S. Atomic Energy Commission.

PION BEAM

The geometry of the beam is shown in Fig. 1. A beryllium target placed 14 deg upstream from a radius through the center of the west straight section was plunged periodically into the path of the circulating proton beam of the Bevatron. Negative pions emitted at zero degrees to the proton beam were deflected 29.95 deg from this beam through a thin window in the vacuum tank. They then passed successively through two standard 8-in. quadrupole triplets, each of which was operated as a single lens. A 5-ft analyzing magnet having a gap of 7-in. then bent the mesons through 7.2 deg into the position occupied by the 30-in. propane bubble chamber. This chamber, which has already been described,[3] is 30-1/2-in. by 21-1/2-in. by 6-1/2-in. It operates in a magnetic field of 13.5 k. gauss.

Trajectories followed by 5.5-Bev/c mesons were computed,[4] and the chamber was placed so that negative pions of this momentum passed down its center. The operation of the quadrupoles resulted in an image of the target at the chamber that was 2.8-in. wide by 1-in. high. The momentum spread was about 80 Mev/c per in. The uncertainty in momentum at any point in the chamber was thus 224 Mev/c. The momentum spread was deduced by the use of wire orbits and counters.[5] Because the beam was concentrated in the region where the momentum was lower than 5.5 Bev/c, the average momentum was lower than this central value. Three methods were used to determine this average. In the first method we combined the observed flux distribution with the momentum distribution across the chamber as determined by the wire orbits. The second method consisted of the direct computation of the average from the curvature measurements of momenta of a series of beam tracks. An elastic constraints program, which is described in more detail later, provided the third determination of the average momentum. The weighted average of the three determinations was 5.17 ± 0.05 Bev/c.

SCANNING

Approximately 11,000 pairs of pictures were scanned on a machine that contains two projectors mounted above a sheet of formica that serves as a viewing screen. Mirrors reflect the light from the projectors on the screen. Because of the nonuniform flux distribution across the chamber, two different fiducial regions were chosen. These are shown in Fig. 2, which contains an outline of the bottom glass of the chamber. Region A, which is bounded by the inner rectangle, is 40 by 30 cm. The outer rectangle bounds region B, which is 50 by 40 cm. Flux was counted on beam tracks that entered region A only, because the large number of tracks between the boundaries of the two regions on the right made the accurate counting of beam tracks in this area very difficult and tedious. The angular distribution, however, contains all observed elastic events whose origins were inside the larger rectangle.

IDENTIFICATION OF EVENTS

Most elastic events at this energy possess certain visual characteristics that permit their tentative identification in the process of scanning. Since this is primarily small-angle scattering, a considerable fraction of the elastic events is expected to have recoil protons that stop in the liquid; we found that 63% of the elastic events had stopping protons. The tracks made by these particles have an ionization which is well above minimum. The scattering angle of the proton is in the neighborhood of 60 to 85 deg, in general. The track of the scattered meson shows minimum ionization and makes a small angle of the order of 2 to 5 deg with the beam pion. The scattering angles were measured roughly with a protractor in the process of scanning, and good agreement with computed values resulted when the scattering plane was fairly flat.

Two slightly different techniques were used to obtain more definite information regarding the identity of the nearly 2000 events that were submitted for measurement. In the first method, the events were classified by imposing the following kinematical conditions that all elastic events must satisfy:

(a) Angular correlation. The incident pion momentum was assigned from the wire orbit calculations according to the location of the event in the chamber, and tables containing the correlated angles as a function of incident momentum were used. The angular correlation of a sample of the elastic events with meson scattering angles of 5 deg or less is shown in Fig. 3.

(b) Correlation of proton range and proton scattering angle for stopping recoils. This requirement is related to (a) and was imposed in the 63% of the cases in which the proton stopped in the liquid. It is the most reliable criterion since the range can be determined with a higher degree of precision, in general, than any of the other parameters.

(c) Coplanarity. This quantity was measured by the angle ψ

between the scattered meson and the plane formed by the incoming meson and the recoil proton. This angle is zero within experimental error for an elastic event.

The requirements of momentum and energy conservation were not imposed, because momentum measurements were not made with sufficient accuracy for these to be meaningful. Since measurements could not be made with infinite accuracy, the above conditions were considered satisfied when the measured angles agreed with the expected ones within experimental errors. For events in which the recoil proton stopped in the liquid, the scattering-angle errors were defined by the equation.

$$\Delta\theta_j = |\theta_t - \theta_f|$$

for $j = m, p$. Here θ_t is the tabulated scattering angle for an elastic event with incoming momentum equal to the wire-orbit value and a proton range equal to the measured value. The angle θ_f is that computed from the geometry of the event. The subscripts m and p stand for the meson and proton, respectively.

The principle sources of errors were: (a) distortions of tracks caused by turbulence in the oil through which the chamber was photographed; (b) errors inherent in the measuring technique (A traveling microscope was used to obtain points along a track in each of the two views. These coordinates, which were punched on IBM cards, permitted the determination of the spatial orientation of the track. The errors associated with this technique involve the accuracy of following a track with the microscope); and (c) multiple scattering affecting curvature and measurements of angles. This latter phenomenon and the oil distortions mentioned above were the primary limitations on the accuracy of momentum measurements. A quantitative study of the errors was made by analyzing the optical system used in photographing events and by repeatedly measuring a series of beam tracks. Following this study, the limiting errors on the measurements of angles of elastic events were assigned as follows: $\Delta\theta_m \leq 2.5$ deg; $\Delta\theta_p \leq 4.5$ deg; $\psi \leq 3.5$ deg.

In the second method of classification of events, the measured scattering angles and momenta were used to define functions $F_\lambda(\theta_j, P_j, P_o)$ that are zero for an elastic event measured with infinite accuracy. This is the method of approximate linear Lagrangian constraints.[6] The F_λ, which are four in number, express momentum unbalance along and transverse to the beam, energy unbalance, and noncoplanarity of a two-prong event. For example, momentum unbalance along the beam direction is expressed by

$$F_1 = P_m \cos\theta_m + P_p \cos\theta_p - P_o .$$

Introducing the Lagrangian multipliers a_λ, one finds the most probable values of the nine quantities associated with a two-prong event (two spatial angles and a momentum described each track) by minimizing

$$M(X_i\, a_\lambda) = \sum_{i=1}^{9} (X_i - X_i^m)^2/u_i + 2\sum_{\lambda=1}^{4} a_\lambda F_\lambda(X_i)$$

The quantities X_i^m are the measured values of the variables, and u_i are the standard deviations assigned to each measured value. These errors are determined from the least-squares fit of a parabola to the projection of the trajectory of a particle on a horizontal plane. Because of the nonlinearity of the constraining equations, the process of minimizing M is actually an iterative one. The values of the functions F_λ for elastic events range from $\sim|10^{-3}|$ to $|10^{-8}|$, while for inelastic events the range is from $\sim|10^{-1}|$ to $|10^{-4}|$. We deduced that a value as large as 50 for M was not unreasonable for an elastic event of poor measurability, and in a few cases even larger values were admitted. We also found that, while inelastic events generally have M values greater than 50, a rather large fraction ($\sim$20%) have values of 50 or less. The distribution in M for the elastic events is shown in Fig. 4. The tail of the distribution is due to elastics having poor quality and to background events indistinguishable from the elastics.

Comparing the results from the two methods, we found that they were in agreement most of the time. In 15% of the cases, however, the conclusions drawn from the two as to the identity of an event were not in agreement. It was found that the assumed errors used in the constraints program were incorrectly estimated in those cases where there was disagreement, and the final decision was made following the more searching study of the errors mentioned previously.

BACKGROUND EVENTS

To check the assignment of maximum-scattering-angle errors for elastic events and also to determine the background from inelastic events, we constructed three error distributions for all events having stopping recoils. In each plot two of the restrictions were invoked on the selected events. Figure 5 shows the $\Delta\theta_p$ distribution for events having ranges of 1 cm or less. All of the events had $\Delta\theta_m \leq 2.5$deg, $\psi \leq 3.5$ deg. The solid curve in the figure represents the gaussian fit to the data obtained when one assumes a limiting error of 4.5 deg on the proton scattering angle of an elastic event. Under the assumption that the background is flat in the acceptance region, it was found that 10% of the accepted events are probably inelastic. Similar plots of the other distributions showed a smaller background when we imposed the same assumption of constant background. This largest effect therefore predominates and fixes the background at 10%.

The assumption of a constant background in the acceptance region was investigated by plotting the three error distribution for inelastic events having stopping recoils. The results are reproduced in Fig. 6. It is seen that the distributions in both $\Delta\theta_m$ and ψ for inelastic events tend to rise in their acceptance regions. This suggests the possibility that background events are likely to have relatively small meson scattering angles, and that the coplanarity of these events is likely to be good by our criteria. The $\Delta\theta_p$ histogram in Fig. 6 shows that the assumption of constant background is, in this case, a good one. Assuming that no strong correlations exist between the three angles for inelastic events, one can define probabilities P_m, P_p, P_c, that the errors in the meson scattering angle, the proton scattering angle, and coplanarity, respectively, of an inelastic event will be less than the corresponding limits for elastic events. At least partial verification of this assumption was obtained by removing the inelastic events in the interval 3 deg $\leq \theta_m \leq 8$ deg. We found that when these same events were removed from the $\Delta\theta_p$ histogram, the shape of the latter was left unchanged. With the large number of reactions that can take place at this energy, and the lack of a one-to-one correspondence between θ_m and θ_p in inelastic events, it is unlikely that strong correlations exist. From the three distributions one obtains: $P_m = 0.428 \pm 0.03$; $P_p = 0.211 \pm 0.01$; $P_c = 0.648 \pm 0.04$.

The probability that an inelastic event simultaneously satisfies the three angular criteria (and is called elastic) is $P_m P_p P_c = 0.058 \pm 0.01$. The final separation of the events yielded 375 elastics and 436 inelastics. The remainder of the measured events were obviously inelastic. The background becomes $436/375 \times 0.068 \sim (7 \pm 3)\%$. The error is larger than statistical and reflects the uncertainty of the limits on the three angles. This figure was used to correct the elastic events for background.

The identity of the elastic events that did not have stopping protons was made by assuming that the measured meson scattering angle was correct to 0.75 deg. A maximum error of 2.5 deg was then allowed on the measured value of the proton scattering angle. These criteria were checked by looking at elastic events in the interval 4 deg $\leq \theta_m \leq 5$ deg. This is the transition region in which some of the recoil protons stop and some do not. Weighting factors were applied to each event in which the recoil stopped. These factors were calculated by assuming azimuthal symmetry around the incoming beam direction, and corrected for events in which the proton would hit one of the physical boundaries of the chamber. By this procedure we estimated that 29 events in the above interval would be expected to have nonstopping protons. By actual count, we had 33 events in which the protons left the chamber. The good agreement between these two numbers means that very little bias was introduced by these criteria.

RESULTS AND CONCLUSIONS

The uncorrected angular distribution of the elastic events is plotted in Fig. 7. The sharp peak in the forward direction is characteristic of diffraction scattering which is, without doubt, the dominant process at this energy. One also observes that no events were found in the backward hemisphere, a result that was reported earlier.[7] This fact is additional evidence for the diffraction nature of the elastic-scattering process at this energy. The corrected angular distribution, represented in Fig. 8 by the circled points, contains only the events for which the meson scattering angles were greater than 6.8 deg in the center-of-mass system. The identification of elastic events was particularly difficult below this angle because the proton recoils are less than 1 cm in length. Multiple scattering and the shortness of the track frequently cause angle measurements to have abnormally large errors. Moreover, many events are missed as one approaches the forward direction from 2 deg because the recoil is too short to be readily observable, if at all. In addition to the correction for background, the observed angular distribution was corrected by a factor of 2% for events missed in both of the two scans of the film. Corrections for the orientation of the scattering planes of the events were computed from Fig. 9 which contains the folded azimuthal distributions of the elastic events. The azimuthal angle ϕ is that between the planes defined by the incident pion and the scattered meson, and the incident pion and the vertical. The ranges on the meson scattering angle in the distributions were chosen so that approximately the same number of events appear in each distribution. Each distribution should be isotropic in ϕ and the observed anisotropy is an indication of the number of events missed. From the histograms, a correction of 32% was deduced for the interval 6.8 deg $\leq \theta^* \leq$ 13.3 deg, while the events observed in the interval 13.3 deg $\leq \theta^* \leq$ 180 deg must be increased by 16%.

In principle, the corrected distribution can be fitted by a cosine series, but the number of parameters that must be determined is prohibitively large. At 5 Bev, one might expect angular momentum states up to $\ell = 10$ to contribute. Furthermore, the observed distribution justifies the use of an optical model. The conventional one was used in which the elastic differential cross section is expressed in the form

$$\frac{d\sigma(\theta^*)}{d\Omega} = a \left| \frac{J_1(b \sin \theta^*)}{b \sin \theta^*} \right|^2 .$$

The solid curve in Fig. 8 is a modified least-squares representation of the corrected data. The constants were determined to be $a = 119.2$mb and $b = 7.78$. From the above equation one finds that the zero occurs for $\theta_m^* = 29.6$ deg, and that $d\sigma(0)/d\Omega$ is 29.8 mb/steradian in the center-of-mass system. This value of the differential cross section is compared in Table I with values deduced from total cross-section data obtained in other experiments. These calculations were made by using the optical theorem, and assuming that the real part of the forward coherent scattering amplitude is negligible at this energy.[8] It is seen that our value is in good agreement with that deduced from the total cross section measurement of Wikner et al.[9] From the above value of b and the wave number in the center-of-mass, $K = 7.46\times10^{13}$ cm^{-1} ± 5%, the pion-proton interaction radius was found to be 1.04×10^{-13} cm ± 5%. This radius is in agreement with that obtained by Steinberger et al., which is $1.08\pm0.06\times10^{-13}$ cm at 1.44 Bev.[10] We are also in agreement with

Table I

σ_T (mb)	Energy (Bev)	$d\sigma(0)/d\Omega$ (mb/sterad)	Reference
30	Extrapolated from lower-energy data to 5.17 Bev	32	Cool, et al.[8]
22.5±2.4	4.7	18±12%	Maenchen et al.[7]
28.7±2.6	4.3	29.1±12%	Wikner et al.[9]
---	5.17	29.8±10%	This measurement.

Maenchen et al., who obtained $(0.9\pm0.15)\times10^{-13}$ cm at 5 Bev. One might conclude on this basis that there is substantially no change in the radius, within experimental error, between 1 and 5 Bev. On the other hand, one wonders whether the lower values observed by Maenchen and by us are indicative of a decrease in this parameter with energy. The possibility that R changes with energy has been previously advanced.[11] One might explain such a decrease crudely by assuming that only the first few angular-momentum states are important, even at high energies. The curve in Fig. 8 was continued beyond the first minimum in order to learn where the second maximum would be expected if diffraction scattering continued to prevail at large angles. The pattern becomes very broad after the first zero, and the second peak occurs at ~43 deg. The differential cross section is only ~0.5 mb/sterad at this peak. These characteristics make the second peak, if it exists, very difficult to observe with these statistics.

The total elastic cross section was calculated from the track length and the total number of events observed in region A of Fig. 2. The track length of 12.22×10^{5} cm was calculated by counting tracks and events in every tenth picture. Contamination from mu mesons was estimated at 4%. The calculation was based on beam geometry and the momentum selection of the steering magnet. An estimate of electron contamination, made by counting the number of electrons that lost 90% or more of their energy in the liquid, resulted in a value of 0.1%. Contamination by electrons is thus negligibly small compared to that from muons. The number of events found in fifucial region A was 237. In addition, 56 events with meson scattering angles in the interval 0 deg $\leq \theta_m \leq 2$ deg were missed. This number was computed from the theoretical curve of Fig. 8. These data yield a total elastic cross section of 5.6±0.5 mb, which is in agreement with the 4.7±1 mb value obtained by Maenchen et al.[7] The assumption that the proton acts like a totally absorbing sphere, however, results in a value of $\pi R^2 = 34$ mb. From the extrapolated value $d\sigma(0)/d\Omega$ and the optical theorem, the total hydrogen cross section was found to be 29.1±10%. The opacity of the sphere is thus 0.69±0.05.

ACKNOWLEDGMENTS

This project was performed through the cooperative efforts of many individuals whose contributions I now gratefully acknowledge. Mr. Larry Oswald played a significant role in the development of the bubble chamber and in its successful operation at the accelerator. This study was undertaken at the suggestion and under the guidance of Professor Wilson Powell. Discussions with Dr. William B. Fowler, Dr. Robert Birge, Mr. John Shonle, and Mr. Zaven Guiragossian were very illuminating. The tasks of data reduction and programming for the IBM 650 were ably performed by Mr. Howard White and his staff. Miss Yuriko Hashimoto spent many hours rescanning the film. To each of these and to the many others who unstintingly gave of their assistance I wish to convey my sincere appreciation.

FOOTNOTES

1. Lattes, Occialini, and Powell, Nature 160, 453 (1947).
2. Fernbach, Serber, and Taylor, Phys. Rev. 75, 1352 (1949).
3. Powell, Fowler, and Oswald, Rev. Sci. Instr. 29, 874 (1958).
4. We are indebted to Mr. Howard White for making these computations.
5. This apparatus was set up by Dr. Robert W. Birge and his staff.
6. Frank T. Solmitz, Data Analysis Development. General Data Analysis I. B. M. Program. Least-Squares Adjustment with Constraints, UCID-153, November 21, 1957.
7. Maenchen, Fowler, Powell, and Wright, Phys. Rev. 108, 850 (1957).
8. Cool, Clark, and Piccioni, Phys. Rev. 108, 1082 (1956).
9. Frederick Wikner, Nuclear Cross Sections for 4.2-Bev Negative Pions (Thesis), UCRL-3639, January 1957.
10. Chretien, Leitner, Samios, Schwartz, and Steinberger, Phys. Rev. 108, 383 (1957).
11. Fowler, Shutt, Thorndike, and Whittemore, Phys. Rev. 103, 1489 (1956).

FIGURE LEGENDS

Fig. 1. The beam geometry.

Fig. 2. Outline of bottom glass of chamber. Region A is bounded by inner rectangle; B, by outer rectangle. The horizontal or vertical distance between two adjacent dots is 5 cm.

Fig. 3. Angular correlation of elastic π-P events. The solid curves show the correlated scattering angles for incident pion momenta of 5 Bev/c and 6 Bev/c, respectively.

Fig. 4. Distribution in M for elastic events.

Fig. 5. Distribution of proton-scattering-angle errors for events having ranges ≥ 1 cm and $\Delta\theta_m \leq 2.5$ deg, $\psi \leq 3.5$ deg.

Fig. 6. Deviations of the scattering angles and coplanarity of background events from values expected for elastic scatters having the same proton ranges.

Fig. 7. Observed angular distribution of the elastic events.

Fig. 8. The corrected angular distribution of the elastic events. The solid curve is that obtained when the proton is pictured as a black sphere.

Fig. 9. Folded azimuthal distributions of elastic events.

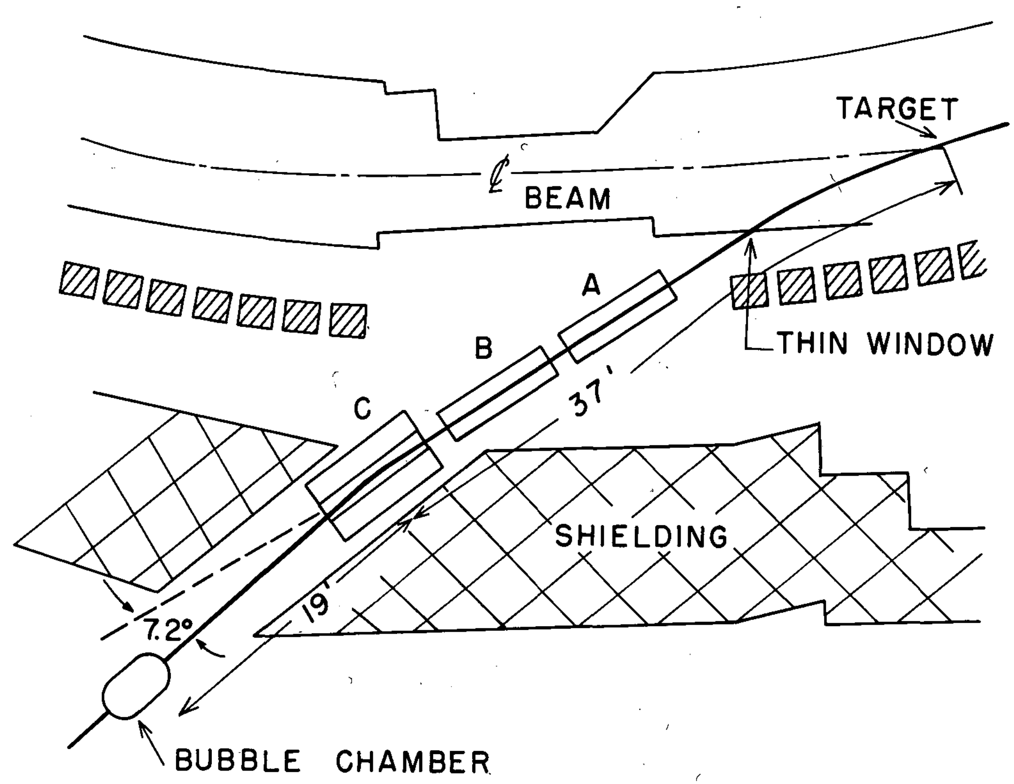
TARGET
BEAM
THIN WINDOW
A
B
C
37'
SHIELDING
19'
7.2°
BUBBLE CHAMBER

Fig 1

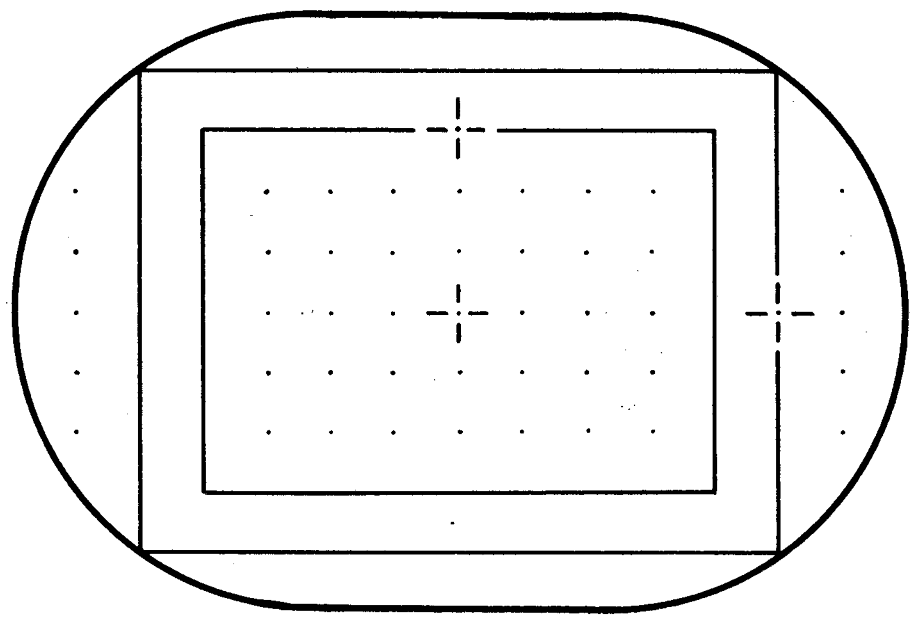

1:1

Fig ~~1~~ 2
56,276-1

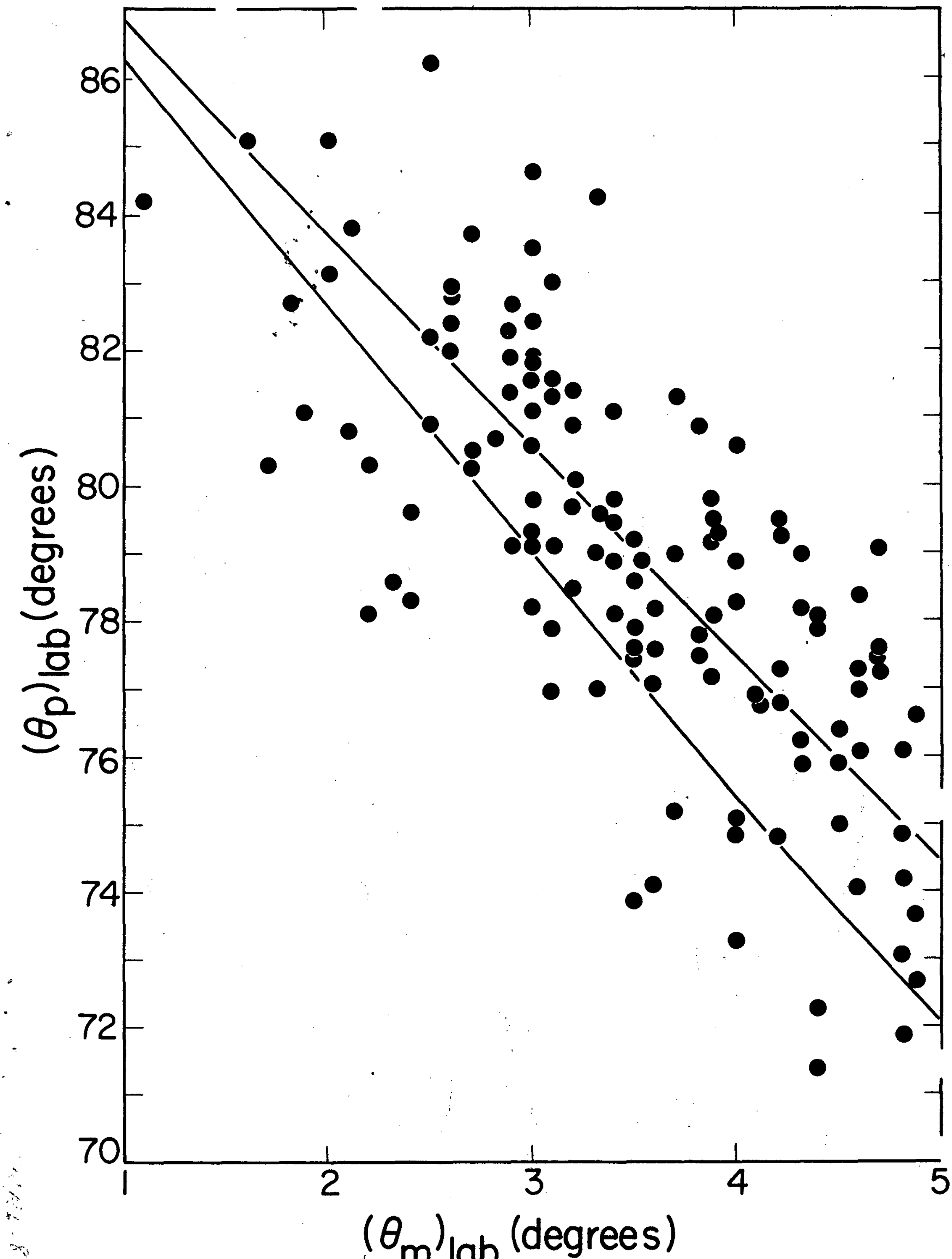

86
84
82
80
78
76
74
72
70
1
2
3
4
5
$(\theta_p)_{lab}$ (degrees)
$(\theta_m)_{lab}$ (degrees)

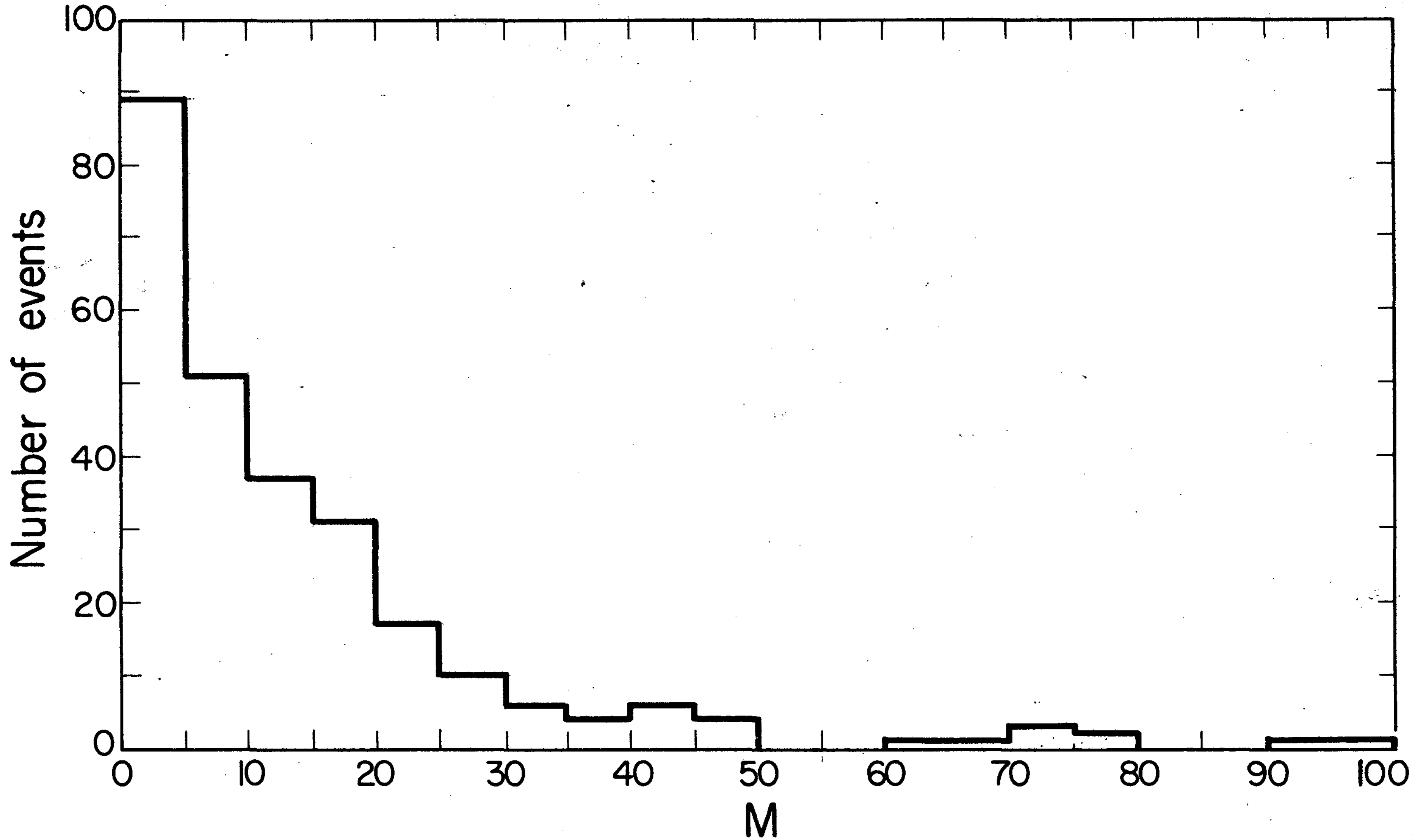

Fig 16

56, 278-1

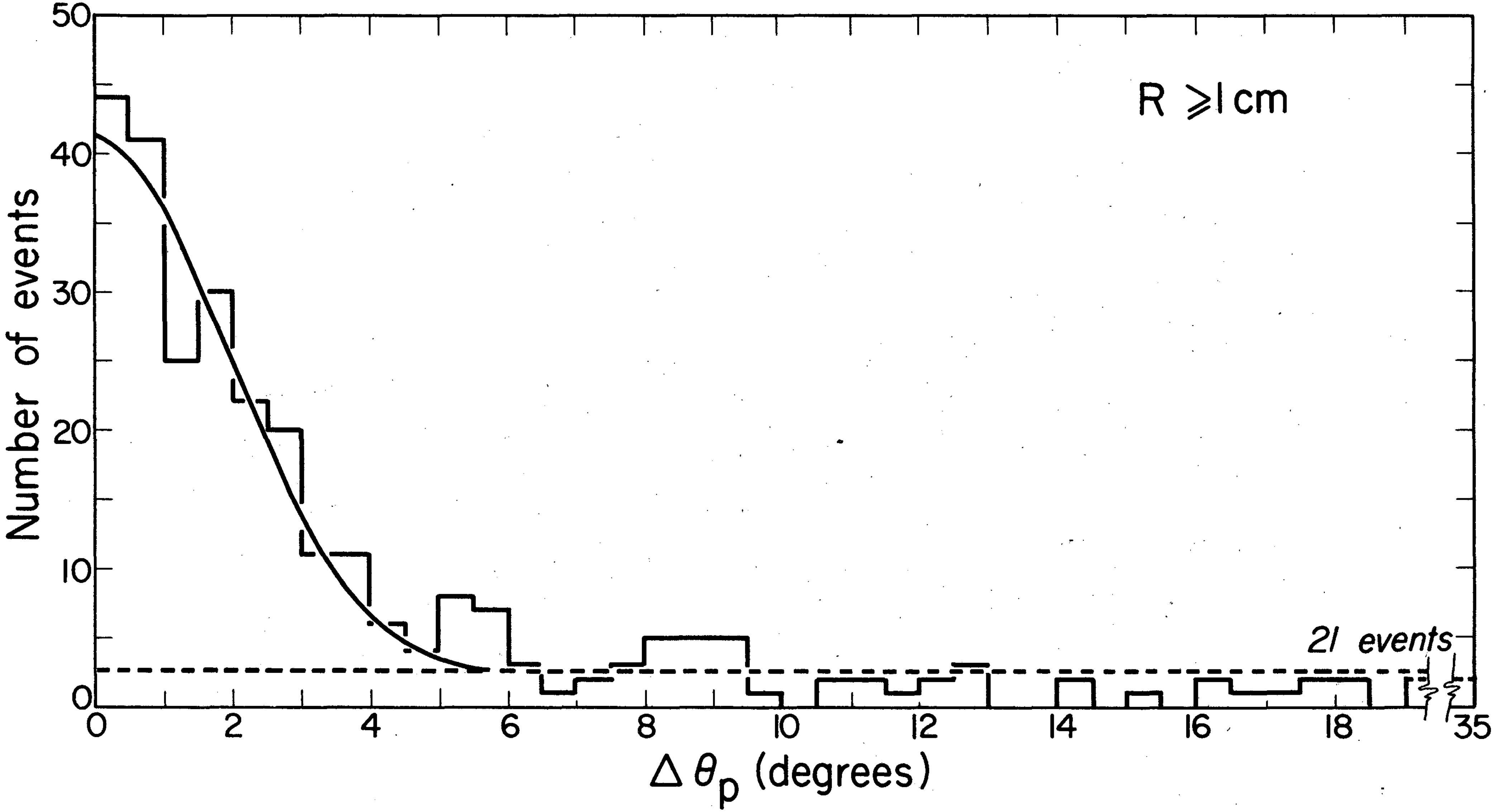

MUB-8165

Fig. 15

56,263-1

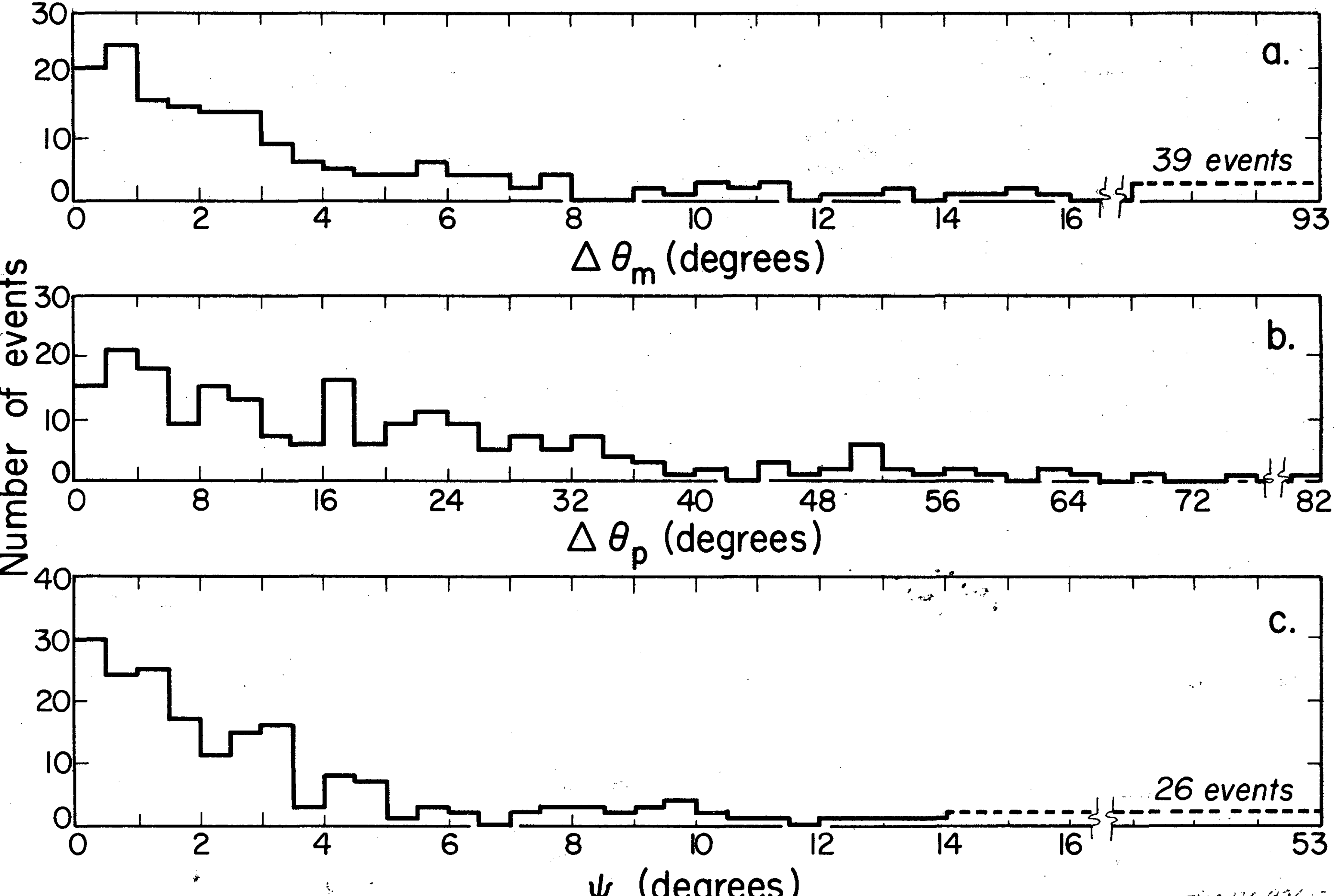

5?

71?RL8?61? 6
Fig ~~21~~

56.272-1 ~~55.103-1~~

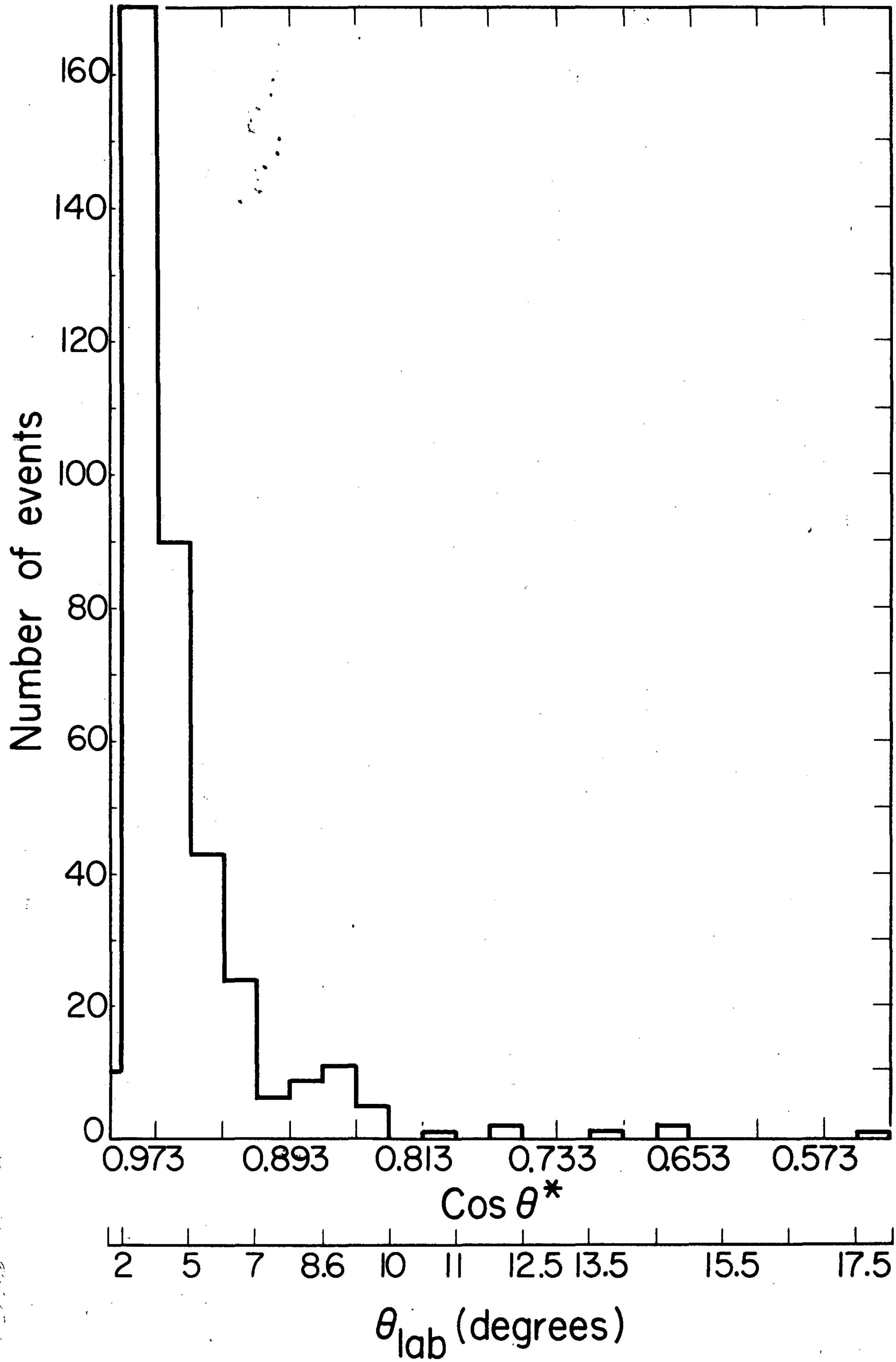

Number of events
160
140
120
100
80
60
40
20
0
0.973
0.893
0.813
0.733
0.653
0.573
Cos θ*
2
5
7
8.6
10
11
12.5
13.5
15.5
17.5
θlab (degrees)

Fig 7

Fig 8

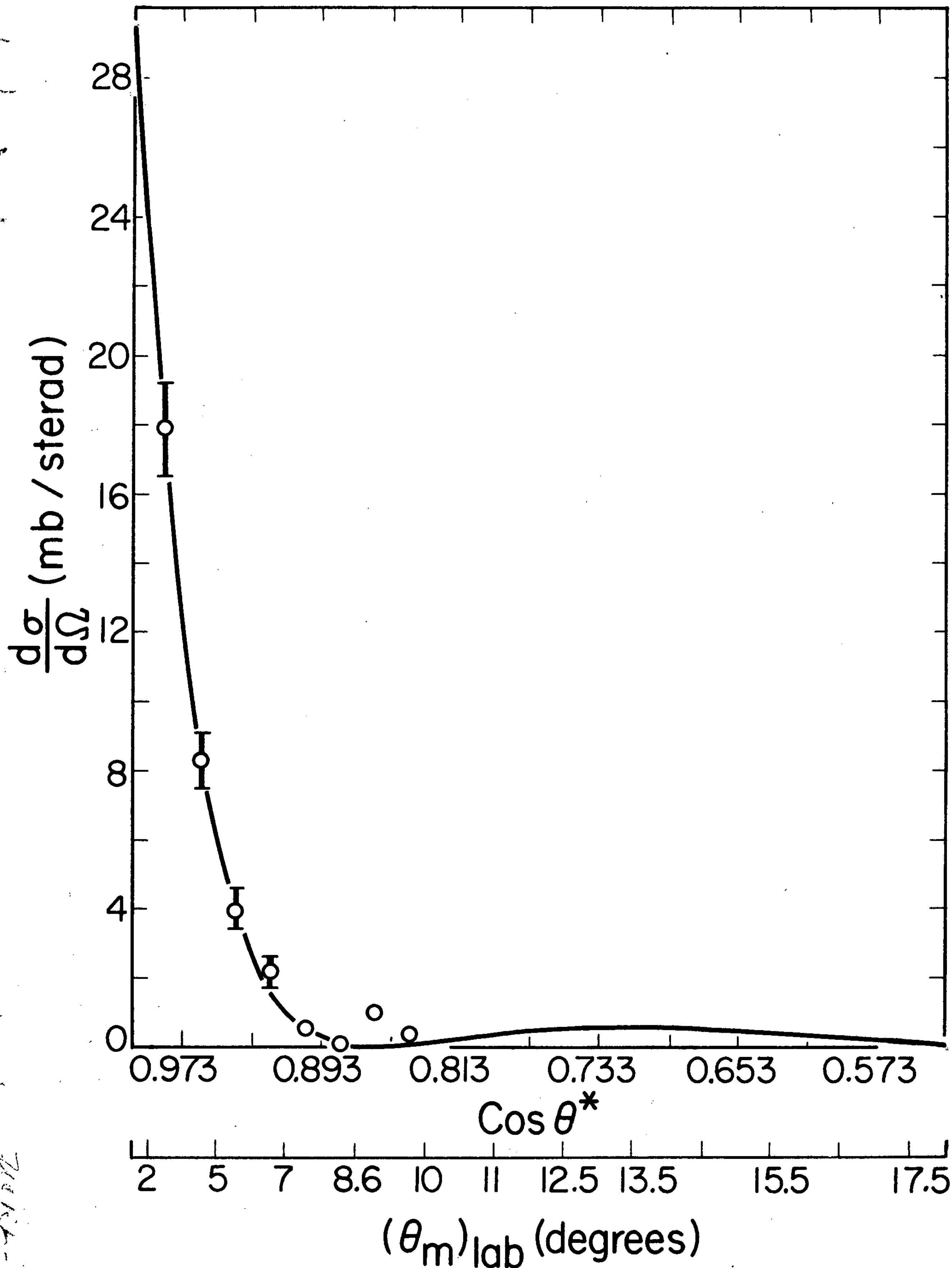

28
24
20
16
12
8
4
0
dσ/dΩ (mb / sterad)
0.973
0.893
0.813
0.733
0.653
0.573
Cos θ*
2
5
7
8.6
10
11
12.5
13.5
15.5
17.5
(θm)lab (degrees)

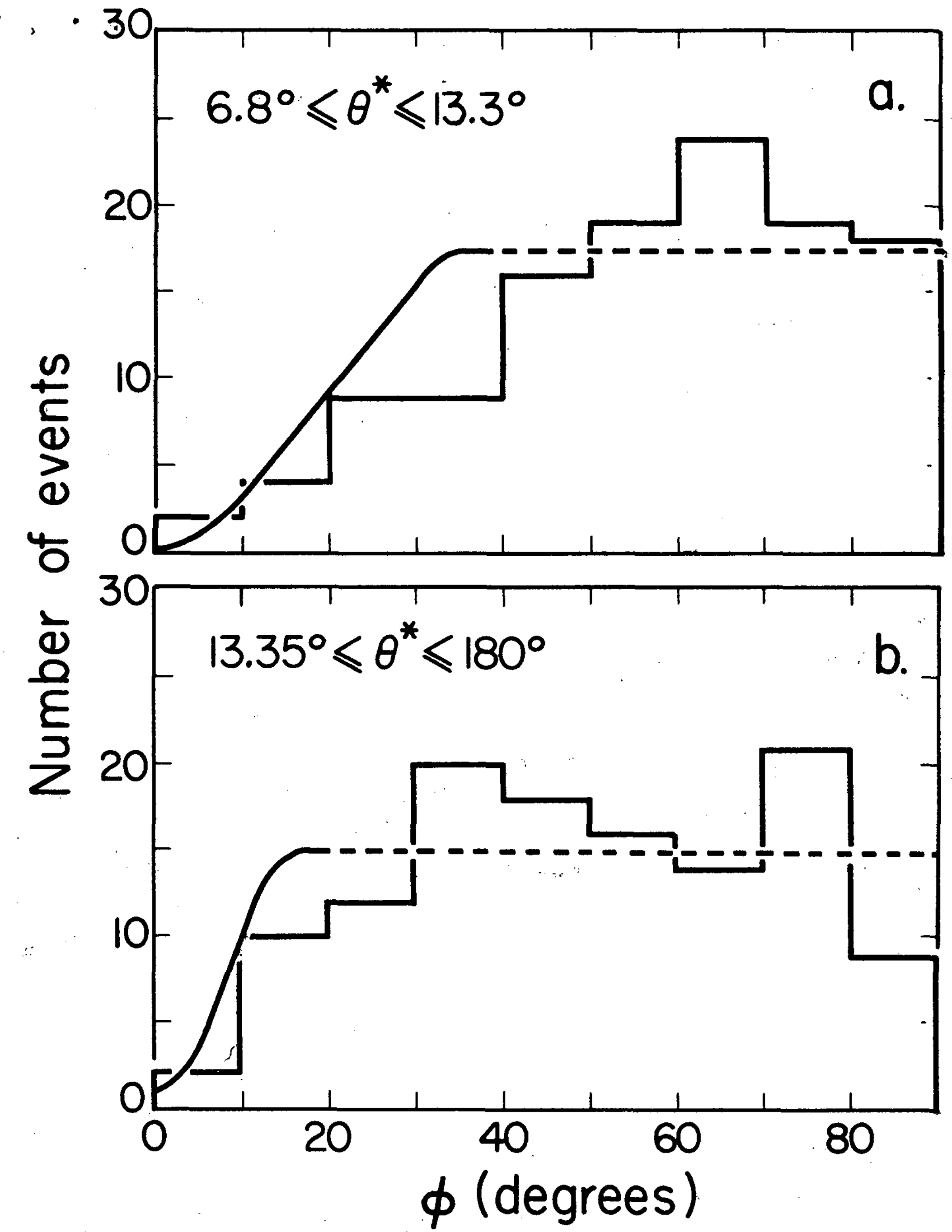
6.8° ≤ θ* ≤ 13.3°
a.
13.35° ≤ θ* ≤ 180°
b.
Number of events
0
10
20
30
0
20
40
60
80
φ (degrees)

Fig. 9

56,264-1